

UDK 661.183.8; 001.572

Cyclic Voltammetric Study of the Influence of Porosity on Electrochemical Response of Nickel-Alumina Modified Glassy Carbon Electrode

Ana Ivanović-Šašić¹, Tatjana Novaković¹, Zorica Mojović^{1*}, Željko Čupić¹, Dušan Jovanović¹

¹University of Belgrade, Institute of Chemistry, Technology and Metallurgy, Department of Catalysis and Chemical Engineering, Njegoševa 12, 11000 Belgrade, Republic of Serbia

Abstract:

Pure and nickel-modified alumina powders with different porosity were synthesized and applied on the glassy carbon electrode by means of Nafion polymer. The data obtained from the nitrogen adsorption-desorption isotherm confirmed that the pore structures in these materials are complex and tend to be made up of interconnected networks of pores of different size and shape. The addition of Ni²⁺ ions caused the changes in the textural properties of the samples. The influence of porosity on the electrochemical behavior of modified electrodes in quasi-reversible process was tested by cyclic voltammetry. Numerical correlations between electrochemical responses of GCE modified with alumina samples and textural properties have been established.

Keywords: Alumina; Textural properties; Voltammetry; Numerical simulation.

1. Introduction

Modified electrodes are extensively used in various fields of electrochemistry such as analytical application, energy storage and conversion. The nature of charge transfer and charge transport processes in these electrodes is usually different from those observed on unmodified planar electrodes. The electrode modified with porous materials, such as alumina [1] has been studied. There are various crystal structures for alumina and the obtained phases depend on the precursor and the calcinations [2, 3]. The surface reactivity, the surface area and pore structure of an alumina phase depends on the preparation conditions, preparation routes and sample history [4, 5]. Polymer-coated electrodes were studied to determine the charge transport mechanism in the coating and for the purpose of catalyzing or mediating redox reactions between the electrode and a substrate in the electrolyte [6, 7]. The electrochemical behavior of redox species incorporated in polymer films has also been studied [8, 9].

In this paper alumina and nickel-modified alumina powders were applied on the glassy carbon electrode by means of Nafion polymer, creating in that manner polymer-modified electrodes with different porosity. The addition of Ni into the alumina sol was expected to create additional diversity in alumina textural properties. The objective of this publication was to investigate the effect of pore structure on electrochemical behavior of redox species incorporated in alumina matrix imbedded in conductive polymer film.

^{*} Corresponding author: zoricam@nanosys.ihtm.bg.ac.rs

Numerical simulations based on Butler Volmer kinetics with 1-dimensional linear diffusion of reduced and oxidized species were used to determine charge transfer rate constant. The obtained electrochemical parameters were correlated with textural properties.

2. Material and methods

Boehmite sol was prepared by the hydrolysis of aluminium isopropoxide according to the procedure given by Yoldas [10]. In order to obtain a Ni(II) doped alumina samples, variable concentration of nickel nitrate solution were mixed with freshly prepared boehmite sol, gelled at 40 °C and thermally treated at temperatures of 500 °C, 900 °C and 1100 °C, during 5h at each temperature. All chemicals were purchased from Sigma-Aldrich. In the designations for pure alumina samples, A stands for alumina and number stands for final temperature (A-500, A-900 and A-1100), while, in the designations for Ni(II) doped alumina samples, first number describes the mass% of Ni in alumina sol and the second number stands for final heating temperature (A10-500, A20-500, etc.).

The nitrogen sorption was performed at -196 °C and relative pressure interval between 0.05 and 0.98 in automatic sorption apparatus (Sorptomatic 1990 ThermoFinnigen). The specific surface areas S_{BET} and C were calculated by the BET method [11, 12] from nitrogen adsorption-desorption isotherms, using data up to $p/p_o = 0.3$, and the pore size distribution have been computed from desorption branch of the isotherms [13].

In order to use the investigated alumina powders as electrode materials, the samples were homogeneously dispersed in original 5 wt.% Nafion® solution using an ultrasonic bath. Droplets (10 μl) of these suspensions (containing 1 mg of alumina powder) were placed on the surface of a glassy carbon electrode (area = 0.0314 cm^2). The alumina-modified glassy carbon electrode (GCE) was used as working electrode. The reference electrode was Ag/AgCl in 3 M KCl, while a platinum foil served as a counter electrode. The electrochemical response of samples was tested by method of cyclic voltammetry in 0.1 M phosphate buffered saline (PBS) at pH 7.0. Furthermore, the obtained alumina and Ni-doped alumina samples were impregnated with saturated solution of potassium ferrocyanide. Such obtained samples were applied to the surface of the glassy carbon electrode in the previously described manner. Cyclic voltammograms were recorded at polarization rate of 50 mVs^{-1} , unless otherwise stated. The polarization rate was varied in the range of 10-1000 mVs^{-1} when the influence of polarization rate was tested. The potential range was -0.3 V to 0.7 V vs. Ag/AgCl reference electrode.

Numerical simulation of CVs was performed using a MatLab program written by Punckt C. [14] based on the algorithm given by Bard and Faulkner [15]. All simulations were performed in one spatial dimension using a system size of 500 μm , a spatial resolution of $\Delta x = 1 \mu\text{m}$, time step of 1×10^{-7} s. Reaction kinetics was defined by the Butler–Volmer equation. We assumed 1-dimensional linear diffusion of reduced and oxidized species with diffusion coefficients of $D_{\text{red}} = 0.8 \times 10^{-12} \text{ m}^2/\text{s}$ and $D_{\text{ox}} = 1.54 \times 10^{-12} \text{ m}^2/\text{s}$, which resemble the transport of the ferrocyanide redox probe.

3. Results and Discussion

3.1. Sorption measurement

Nitrogen adsorption-desorption isotherms of all samples (Fig. 1 a,c,d) expressed isotherm type IVa behavior, characteristic for low porosity material or material with mostly mesoporous pore diameters, as was the case with samples investigated in this paper.

As well as many inorganic gels most of these samples (except A-1100 and A10-1100) gave the Type H2 hysteresis loops. The pore structures in these materials were complex and

tend to be made up of interconnected networks of pores of different size and shape (Fig. 1 b,d,f). Only isotherms of two samples (A-1100 and A10-1100) had a hysteresis loop of the H1 type, originally known as Type A, which is a fairly narrow loop with very steep and nearly parallel adsorption and desorption branches given by adsorbents with a narrow distribution of uniform, cylindrical pores. The changes in the structure cause the changes in the textural properties of the samples (Tab. I).

The observed changes of textural properties obtained for the samples calcined at higher temperatures were the result of the sintering process. Addition of Ni (II) ions caused decrease in specific surface area, pore volume and mean pore diameter compared to pure alumina samples, calcined at equal temperature. It was also noted that the samples with the addition of nickel are more resistant to change due to sintering at elevated temperatures, compared to those without the additive. Some deviations such as pore diameter of 52 nm for A-1100 sample and somewhat unusual isotherm of A10-1100 sample have been observed and cannot be explained at the moment.

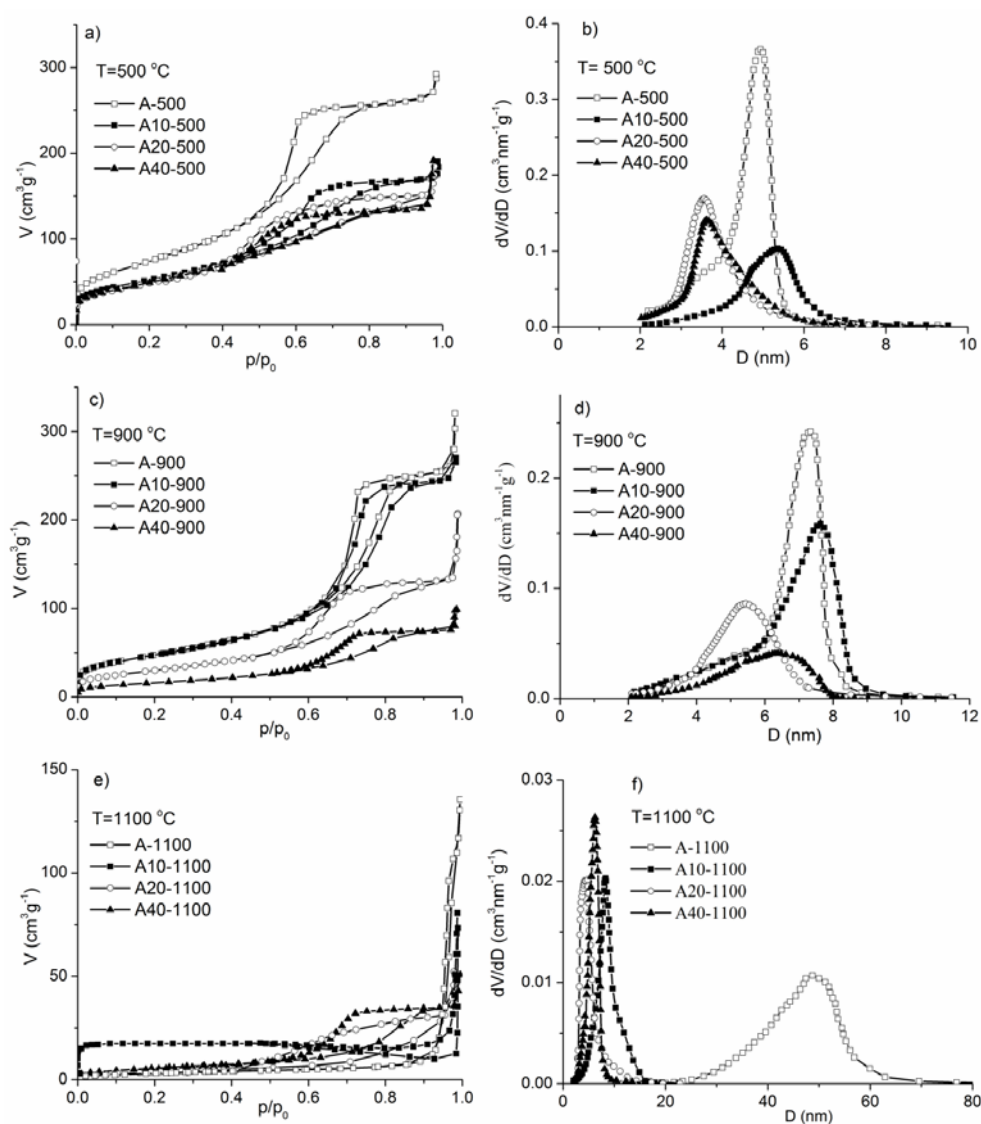


Fig. 1. N₂ adsorption/desorption isotherms (a,c,e) and pore size distribution (b,d,f) for alumina and nickel-doped alumina samples calcined at different temperatures.

Tab. I Textural properties of alumina samples, pure and doped with Ni²⁺ calcined at 500, 900 and 1100°C.

Sample	S _{BET} (m ² g ⁻¹)	V _{p0.98} (cm ³ g ⁻¹)	V _{p micro} (cm ³ g ⁻¹)	D _{max} (nm)	Type of isotherm and hysteresis loop
A-500	280	0.441	0.104	4.9	IVa, H2
A10-500	190	0.272	0.075	5.3	IVa, H2
A20-500	183	0.281	0.057	3.6	IVa, H2
A40-500	173	0.227	0.063	3.6	IVa, H2
A-900	174	0.472	0.062	7.3	IVa, H2
A10-900	170	0.414	0.063	7.8	IVa, H2
A20-900	110	0.241	0.042	5.4	IVa, H2
A40-900	58	0.124	0.021	6.5	IVa, H2
A-1100	12	0.162	0.004	52	IVa, H1
A10-1100	29	0.096	0.012	8.3	IVa, H1
A20-1100	14	0.078	0.005	4.3	IVa, H2
A40-1100	23	0.065	0.009	6.2	IVa, H2

where S_{BET} is specific surface area; V_{p0.98} is total pore volume estimated from the amount of nitrogen adsorbed at the relative pressure of 0.98; V_{p micro} is micropore volume; D_{max} is the maximum pore diameter

3.2. Electrochemical behavior

All Nafion/alumina coated electrodes produced cyclic voltammograms of similar shapes with very low current (not presented) without any distinct features. Recorded cyclic voltammograms exhibited different level of sloping that is characteristic of porous materials [16].

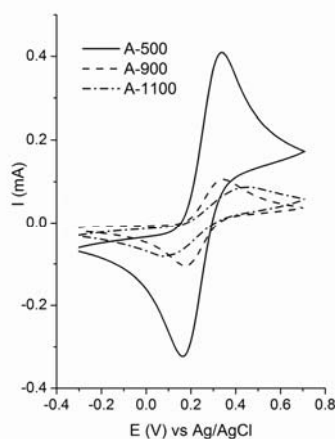


Fig. 2. Cyclic voltammograms of GCE modified with alumina powders with incorporated ferrocyanide ions recorded in 0.1 M phosphate buffered saline at pH 7.0, recorded at polarization rate of 50 mVs⁻¹.

Further experiment consisted of investigating the electrochemical response of redox probe, ferrocyanide ion, incorporated within different alumina samples. Prior this, the behavior of bare GCE in saturated potassium ferrocyanide solution in 0.1 M PBS was investigated. Also, the behavior of Nafion film containing trapped potassium ferrocyanide powder in 0.1 M PBS was investigated. Diffusion coefficients of ferrocyanide ion in PBS solution and through Nafion were assessed by Randles-Sevcik equation [BARD]. The values of diffusion coefficients of ferrocyanide obtained for PBS solution and Nafion were 2.2x10⁻⁶ cm²s⁻¹ and 1.5x10⁻⁸ cm²s⁻¹, respectively, what is in good agreement with literature data [17, 18].

Voltammograms of all ferrocyanide impregnated alumina samples were recorded in PBS at pH 7.0. General shape of CV obtained for investigated samples is presented at Fig. 2. The rest of CV was omitted for the sake of clarity.

Cyclic voltammograms can be characterized by the peak current and the peak-to-peak separation (ΔE_p) and these values are presented in Tab. II.

Additional data can be obtained from cyclic voltammograms. The Tafel slope (b) could be obtained from the slope of peak potential vs. log (scan rate) [15]. The other manner to obtain Tafel slope is from slope of Tafel mass transfer-corrected plot (E vs. $\log(I_k)$, where $I_k = (I^* I_L) / (I_d - I)$ and $I_L / (I_L - I)$ is the mass transfer correction) [15]. Tafel slopes obtained in these two manners are also presented in Tab. II. The cyclic voltammograms recorded at different polarization rate for sample A-500 are presented at Fig. 3.

Tab. II The data obtained from voltammograms of alumina samples impregnated with ferrocyanide ion recorded in 0.1 M PBS.

Sample	I_a (μA)	I_c (μA)	ΔE_p (mV)	Tafelslope ^a (mV dec ⁻¹)	Tafelslope ^b (mV dec ⁻¹)
A-500	332	339	167	84 + 190	63
A10-500	200	220	223	119+ 188	68
A20-500	305	319	259	107+ 247	61
A40-500	292	311	175	133+260	66
A-900	94	110	167	160	62
A10-900	57	65	127	120	54
A20-900	55	64	191	150	65
A40-900	34	39	191	185	67
A-1100	58	77	317	158	94
A10-1100	40	48	231	142	83
A20-1100	43	55	325	153	96
A40-1100	17	20	207	140	76

where I_a and I_c are anodic and cathodic peak current, respectively, ΔE_p is the difference between anodic and cathodic peak potential, ^a calculated from $E_p = f(\log v)$, ^b calculated from mass-transfer corrected current

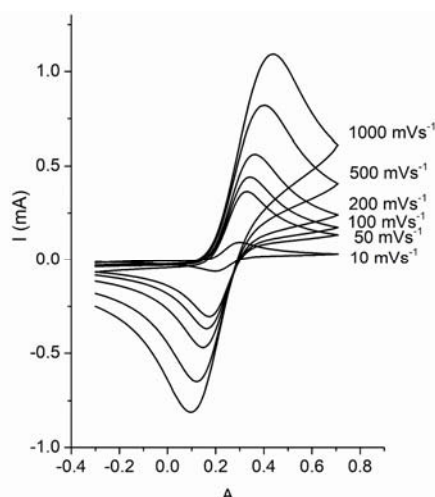


Fig. 3. Cyclic voltammograms A-500 sample with incorporated ferrocyanide ions recorded in 0.1 M phosphate buffered saline at pH 7.0 at different polarization rates (10-1000 mVs⁻¹).

Some of Tafel slopes obtained by dependence on scan rate showed two values of Tafel slopes in investigated range of scan rates, while some voltammograms exhibited only one slope. Tafel values obtained in this manner for bare GCE in saturated ferrocyanide

solution and GCE covered with Nafion containing ferrocyanide were 124 mV dec^{-1} and 242 mV dec^{-1} , respectively. The values of Tafel slope obtained by mass-transfer correction for series of samples calcined at $500 \text{ }^\circ\text{C}$ and $900 \text{ }^\circ\text{C}$ were in good agreement with expected slope of 59 mV dec^{-1} for two-electron process. The values obtained for series of samples calcined at $1100 \text{ }^\circ\text{C}$ were higher than expected indicating the presence of additional polarization resistance. Tafel values obtained in this manner for bare GCE in saturated ferrocyanide solution and GCE covered with Nafion containing ferrocyanide were 67 mV dec^{-1} and 116 mV dec^{-1} , respectively.

With increase of calcination temperature the shape of voltammogram shifted toward more irreversible behavior (i.e. increased ΔE_p values), indicating change of the charge transfer rate constant (k_s) value of the system. Numerical simulation was employed to determine k_s for oxidation of ferrocyanide ion and reduction of formed ferricyanide ion and respective transfer coefficients. The obtained results for rate constants and transfer coefficients are given in Tab. III. Recorded cyclic voltammogram is compared with numerical simulation in Fig. 4. Although simulations were not ideally fitted to the experimental curves, positions of the current peak maxima and curve shapes are quite satisfactory.

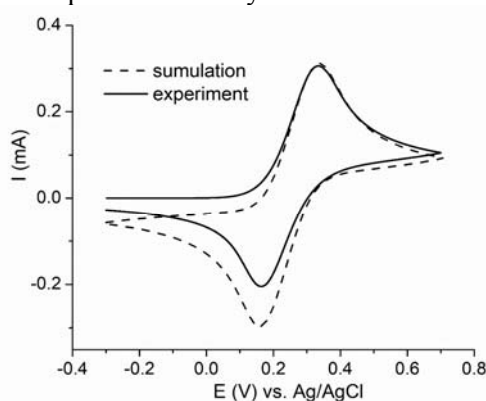


Fig. 4. Recorded (solid curve) and simulated (dashed curve) cyclic voltammogram for sample A10-500 with incorporated ferrocyanide ions. Experimental CV was recorded at polarization rate of 50 mVs^{-1} .

Tab. III Data obtained by numerical simulation.

Sample	$k_a \text{ (m s}^{-1}\text{)}$	α_a	$k_c \text{ (m s}^{-1}\text{)}$	α_c
A-500	$2\text{e-}7$	0.33	$2\text{e-}6$	0.35
A10-500	$1\text{e-}7$	0.35	$1.7\text{e-}6$	0.41
A20-500	$1.3\text{e-}7$	0.40	$2.8\text{e-}6$	0.42
A40-500	$1.3\text{e-}7$	0.40	$2.8\text{e-}6$	0.42
A-900	$2\text{e-}7$	0.35	$3\text{e-}6$	0.35
A10-900	$2\text{e-}7$	0.40	$4\text{e-}6$	0.35
A20-900	$1\text{e-}7$	0.40	$2\text{e-}6$	0.35
A40-900	$1\text{e-}7$	0.40	$2\text{e-}6$	0.35
A-1100	$0.8\text{e-}7$	0.25	$1\text{e-}6$	0.30
A10-1100	$4\text{e-}7$	0.30	$4\text{e-}7$	0.30
A20-1100	$0.6\text{e-}7$	0.25	$8\text{e-}7$	0.30
A40-1100	$2\text{e-}7$	0.30	$2\text{e-}6$	0.30
GCE	$8\text{e-}7$	0.35	$1\text{e-}4$	0.35

k_a and k_c – rate constants for oxidation and reduction process, respectively, α_a and α_c – transfer coefficient for oxidation and reduction process

The method of multiple correlation analysis was performed on obtained experimental

results in order to show the strength of the relationship between the examined variables. Presented correlation matrix (Tab. IV) does not contain the values of sample A-1100 because of their large deviation and this sample was disregarded from analysis. Since the analyzed results were experimentally obtained, correlation coefficient equal or greater than 0.7 was considered as significant. The representative dispersion diagram is presented at Fig. 5. The obtained correlation factor was -0.70729, while adjusted R-square (R^2) amounted 0.44473.

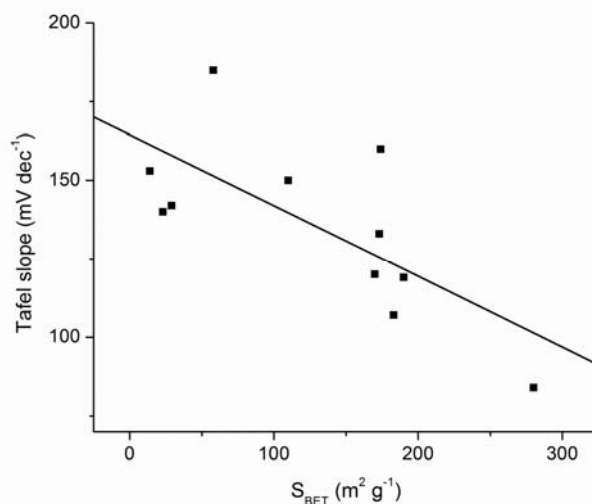


Fig. 5. The representative dispersion diagram of Tafel slope^{a1} (obtained without mass-transfer correction at low overpotentials) with specific surface area, obtained by the method of multiple correlation analysis.

Tab. IV Correlation matrix of analyzed variables.

	I_a (mA)	I_c (mA)	ΔE_p (mV)	Tafel slope ^{a1}	Tafel slope ^{a2}	Tafel slope ^b	k_a ($m s^{-1}$) ^d	α_a^c	k_c ($m s^{-1}$) ^d	α_c^c
S_{BET}	0.80	0.80	-0.50	-0.71	0.44	-0.74	-0.10	0.46	0.56	0.68
$V_{p0.98}$	0.46	0.47	-0.62	-0.47	0.08	-0.76	0.02	0.41	0.68	0.41
$V_{p\ micro}$	0.77	0.77	-0.53	-0.70	0.39	-0.72	-0.09	0.43	0.52	0.64
D_{max}	-0.67	-0.67	-0.41	0.33	-0.76	-0.07	0.67	-0.09	0.00	-0.55

^a calculated from $E_p = f(\log v)$ (1 - for low overpotentials; 2 - for high overpotentials)

^b calculated from mass-transfer corrected current

^c obtained by numerical simulation

The positive correlation of peak current, both anodic and cathodic, was established with specific surface area and micropore volume. The samples were soaked with saturated solution of potassium ferrocyanide up to their maximum uptake of solution. Therefore, the effect can be attributed to the preconcentration effect of the porous materials, as is well known for zeolite-modified electrodes [37]. The negative correlation of peak currents with D_{max} , as well as low correlation coefficient with total pore volume, might indicate that the effect of mesopores was less significant than the effect of micropores.

The expected Tafel slope for one electron transfer is 120 mV/decade. However, the Tafel slope obtained for bare GCE amounts 67 mV/decade, indicating that at investigated conditions, two-electron transfer occurred. This conclusion is in accordance with the fact that at high concentrations of ferrocyanide ions, ion pairing is increased [19]. Having this in mind it can be concluded that investigation of Tafel slope for porous electrode should be performed with mass-transfer correction. Negative correlation of mass-transfer corrected Tafel slope with specific surface area, total pore volume and micropore volume was established. Increased Tafel slope with decrease of this parameters indicated that additional polarization resistance arise probably due to diffusion restriction. On the other hand, Tafel slope obtained

without mass-transfer correction showed negative correlation with specific surface area and micropore volume for low overpotential, while for high overpotential negative correlation was obtained with D_{\max} . Although non-corrected Tafel slope values were not reliable, this correlations indicated that at low overpotentials the electrode behavior was more influence by micropores, while at high overpotentials mesopores were more important.

The obtained k values for carbon glass electrode modified with investigated samples were smaller than value obtained for bare GC electrode. However, no correlation of oxidation rate constants (k_a) and anodic transfer coefficient (α_a) was established with textural properties. The variation of k_a can be ascribed to different coverage of the electrode by the applied alumina samples since the determined value of k is product of $(1-\theta)$ and k at active sites, where θ is surface coverage. Higher coverage is expected for samples with lower porosity. However, it seems that resulting coverage is more result of random distribution of particles on the electrode surface than of the porosity of sample. On the other hand, certain correlation trend was noticed for reduction rate constants (k_c) and cathodic transfer coefficient (α_c). These correlations indicated that porosity of alumina samples influenced the behavior of formed ferricyanide ions.

Porous aluminum oxide gels, as well as other porous materials as zeolites and clays, are used as matrices for immobilization of electroactive species at the electrode surface. The investigation of these systems is often performed by cyclic voltammetry. The properties of recorded voltammograms depended on the textural properties of used alumina. The assessment of the obtained results should be performed having in mind that the obtained results might be due to limitations imposed by matrices rather than kinetic response of the investigated electroactive species.

4. Conclusion

Pure and nickel-doped alumina powders were synthesized in order to obtain series of material with different textural properties. The nitrogen sorption data confirmed mesoporosity of obtained materials and that structural properties affect the texture of the samples. The synthesized materials were impregnated with saturated ferrocyanide solution and used to modify glassy carbon electrode by means of Nafion. The electrochemical behavior of modified electrodes was tested in phosphate buffer by cyclic voltammetry. The analysis of recorded cyclic voltammograms revealed that peak current depended on pore volume, probably through effect of preconcentration. Tafel analysis performed with mass transfer correction gave more reliable data. Charge transfer rate constant was estimated by numerical simulation. The values of charge transfer rate constant obtained for GCE covered with investigated samples were lower than value obtained for bare GC electrode. This was the consequence of coverage of the electrode by alumina powder and no significant correlation between electrochemical response and textural parameters could be notice for the forward reaction i.e. ferrocyanide ion oxidation. On the other hand, certain correlation trend was noticed for reduction rate constants (k_c) and cathodic transfer coefficient (α_c). These correlations indicated that porosity of alumina samples influenced the behavior of formed ferricyanide ions. The efficiency of investigated electrocatalytic process depended on the interplay of mass transport and electron transport influenced by the chemical and physical structure of the alumina immobilized in Nafion matrix.

Acknowledgment

This work was supported by the Ministry of Education, Science and Technological Development of the Republic of Serbia, (Project Nos. III 45001 and ON 172015).

5. References

1. C. J. Miller, M. Majda, Anal. Chem., 60 (1988) 1168.
2. J. Xu, A-R. Ibrahim, X. Hu, Y. Hong, Y. Su, H. Wang, J. Li, Micropor. Mesopor. Mat., 231 (2016) 1.
3. M. Spataru, M. Muntean, Sci. Sinter., 35 (2003) 37.
4. X. Chen, Y. Liu, G. Niu, Z. Yang, M. Bian, A. He, Appl. Catal. A-Gen., 205 (2001) 159.
5. Z. Zhihui, L. Nan, R. Guozhi, Sci. Sinter., 39 (2007) 9.
6. N. Oyama, F.C. Anson, J. Electrochem. Soc., 127 (1980) 247.
7. R. A. Bull, F.-R. F. Fan, A. J. Bard, J. Electrochem. Soc., 129 (1982) 1009.
8. T. P. Henning, A. J. Bard, J. Electrochem. Soc., 130 (1983) 613.
9. P. Bertocello, I. Ciani, F. Li, P. R. Unwin, Langmuir, 22 (2006) 10380.
10. B. E. Yoldas, Am. Ceram. Soc. Bull., 54 (1975) 286.
11. F. Rouquerol, J. Rouquerol, K. S. W. Sing, P. Llewellyn, G. Maurin, Adsorption by powders and porous solids: Principles, methodology and applications, Academic Press, New York, 2012.
12. B. C. Lippens, B. G. Linsen, J. H. de Boer, J. Catal., 3 (1964) 32.
13. K. Sing, D. Everet, R. Haul, L. Moscou, R. Pierotti, J. Rouquérol, T. Siemieniowska, Pure Appl. Chem., 57 (1985) 603.
14. C. Punckt, M. A. Pope, I. A. Aksay, J. Phys. Chem., C 117 (2013) 16076.
15. A. J. Bard, L. R. Faulkner, Electrochemical Methods, Fundamentals and Applications, second ed., John Wiley & Sons, New York, 2001.
16. D. R. Rolison, The intersection of electrochemistry with zeolite science, in: J.C. Jansen, M. Stöcker, H.G. Karge, J. Weitkamp (Eds.), Advanced Zeolite Science and Applications, Elsevier, Amsterdam, The Netherlands, 1994, pp. 544-587.
17. H-C. Chang, C-C. Wu, S-J. Ding, I-Shiun Lin, I-Wen Sun, Anal. Chim. Acta, 532 (2005) 209.
18. D. De Wulf, A.J. Bard, J. Macromol. Sci. Part A - Chem., 26 (1989) 1205.
19. R. Noufi, D. Tench, L. F. Warren, J. Electrochem. Soc., 128 (1981) 2363.

Садржај: Синтетисани су прахови чисте и никл-модификоване алумине различите порозности и постављени на површину електроде од стакластог угљеника посредством Нафиона. Подаци добијени из адсорпционо-десорпционих изотерми азота су потврдили да је порозна структура у овим материјалима сложена и да је сачињава повезана мрежа пора различитих различитих величина и облика. Додатак Ni^{2+} јона је проузроковао промену текстуалних својстава узорака. Утицај порозности на електрохемијско понашање модификованих електрода у квази-реверзибилном процесу је тестиран цикличном волтаметријом. Нумеричке корелације између електрохемијског одговора електроде од стакластог угљеника модификоване узорцима алумине и текстуалних особина су установљене.

Кључне речи: Алумина; текстуална својства; волтаметрија; нумеричка симулација.

